JOURNAL OF APPLIED ELECTROCHEMISTRY 23 (1993) 966–974

Effect of mass transfer on the current distribution in monopolar and bipolar electrochemical reactors with a gas-evolving electrode

J. M. BISANG

Programa de Electroquímica Aplicada e Ingeniería electroquímica (PRELINE), Facultad de Ingeniería Química, Universidad Nacional del Litoral, Santiago del Estero 2829, 3000 Santa Fe, Argentina

Received 30 June 1992; revised 8 October 1992

The current distribution in an electrochemical reactor with vertical parallel-plate electrodes was experimentally determined. The research was performed with monopolar and bipolar electrodes. The reactor has a gas-evolving electrode and at the counter electrode an electrochemical reaction with combined diffusion and charge-transfer kinetic control, takes place. Therefore the kinetics at the counter electrode are influenced by the bubble-induced convection and by the forced convection of the electrolyte. These reactors are found in many electrochemical processes, for example, electrowinning of metals and electrosynthesis. The test reactions were hydrogen evolution at the cathode and the anodic oxidation of sulphite to sulphate from basic solutions. The current distribution shows a minimum at a distance of approximately six times the equivalent diameter of the reactor from the inlet region. This minimum is a consequence of the interaction between forced convection and the bubble-induced convection, which shifts the mass transfer coefficient of the anodic reaction along the reactor. The effects of the total current, the volumetric electrolyte flow rate and the metal phase resistance on the current distribution are also analysed. The experimental current distribution data are compared with theoretical expectations and good agreement is found.

Nomenclature

b_i constant in the Tafel equation for the ith reaction $= \alpha\nu_{e,i}F/RT$ (V^{-1})
C concentration (mol cm^{-3})
D diffusion coefficient (cm^2 s^{-1})
e_i thickness of the ith electrode (cm)
E electrode potential (V)
E_0 reversible electrode potential (V)
F Faraday constant (A s mol^{-1})
g gravitational acceleration (cm s^{-2})
i current density (A cm^{-2})
i_d limiting current density (A cm^{-2})
$i_{d,i}$ limiting current density in the ith reactor (A cm^{-2})
i_k kinetically limited current density (A cm^{-2})
i_0 exchange current density (A cm^{-2})
I total current (A)
K mass-transfer coefficient (cm s^{-1})
K_b bubble-induced mass-transfer coefficient (cm s^{-1})
K_c convective mass-transfer coefficient (cm s^{-1})
L electrode length (cm)
n number of bipolar electrodes
P gas pressure (atm)
Q volumetric liquid flow rate (cm^3 s^{-1})
R gas constant (atm cm^3 K^{-1} mol^{-1})
S interelectrode distance (cm)
T temperature (K)
U_0 reversible cell voltage (V)
v_g^0 superficial gas flow velocity (cm s^{-1})
v_l^0 superficial liquid flow velocity (cm s^{-1})
v_s single bubble rise velocity (cm s^{-1})
v_{sw} bubble swarm rise velocity (cm s^{-1})
V applied voltage to the reactor (V)
W electrode width (cm)
y axial coordinate (cm)

Greek characters

$\bar{\delta}_r$ mean relative deviation
$\Delta\phi_{m,i}$ ohmic drop in the metal phase of the ith electrode (V)
$\Delta\phi_{s,i}$ ohmic drop in the solution phase of the ith reactor (V)
ϵ gas voidage
ϵ_m limiting gas voidage
$\eta_{a,i}$ anodic overvoltage at the ith electrode (V)
$\eta_{c,i}$ cathodic overvoltage at the ith electrode (V)
ν kinematic viscosity (cm^2 s^{-1})
$\nu_{e,i}$ charge number of the ith electrode reaction
ρ electrolyte resistivity (Ω cm)
ρ_m metal phase resistivity (Ω cm)
σ population standard deviation
ϕ_m metal phase potential (V)

Subscripts

A terminal anode in the bipolar stack
B_i ith bipolar electrode
C terminal cathode in the bipolar stack

0021-891X

1. Introduction

The current distribution in electrochemical reactors with parallel-plate electrodes has been studied by many authors. Tobias [1] considered the effect of gas evolution on the ohmic resistance and on the current distribution in electrolysers with stationary electrolyte. Funk and Thorpe [2] took into account the flow of the solution phase and introduced the concept of the slip ratio. Nishiki *et al.* [3] also studied a cell under forced convection conditions but assuming that the slip ratio was unity and considering the overpotential at the working electrode of the linear type and of the Butler–Volmer type. Rousar *et al.* [4, 5] developed models for monopolar electrochemical reactors taking into account all the terms in the voltage balance equation and proposed a simplified model for electrolysers with a small electrode height, small current density and high flow rate. Likewise, in [4] and [6] the mathematical model was extended to bipolar electrochemical reactors. The ohmic drop in the metal phase of the bipolar electrode was incorporated into the model but a one-dimensional current flow in the electrode was considered. A linearized equation was used for the kinetic electrode.

Based on the coalescence barrier model [7], Martin and Wragg [8] analysed the current distribution in electrochemical reactors with different configurations. The present author reported theoretical and experimental studies of current distribution in a monopolar reactor with gas-evolving electrodes [9]. Likewise, current distribution data in a tall vertical gas-evolving cell were recently reported in [10] and, for a hypochlorite cell, in [11].

In the above work, the electrochemical reactions at both electrodes are considered to be charge-transfer kinetic controlled. However, in many electrochemical processes such as the electrodeposition of metals, onsite hypochlorite generation, production of redox mediators for indirect electrosynthesis etc, electrochemical reactors with vertical electrodes are used where, at one electrode a reaction influenced by mass-transfer occurs and the counter electrode evolves a gas. Therefore, the current distribution in the reactor is influenced mainly by the gas generation, which produces a variation of the effective electrolyte resistivity with axial position and also alters the mass-transfer coefficient of the electrochemical reaction at the working electrode. Likewise, in most cases forced convection is superimposed on the bubble-induced convection so that the current distribution is also influenced by the electrolyte flow.

On the other hand, in many electrochemical processes bipolar arrangements are adopted, which produce a variation in the current distribution with respect to the monopolar case mainly due to the effect of the electrolyte resistances incorporated in series. With respect to bipolar electrodes Scott [12] has theoretically analysed the effect of the electrode resistance on the current distribution in bipolar parallel-plate electrodes using a one-dimensional mathematical model, the electrochemical characteristics of each cell being represented by a pure resistance. Divisek [13] has taken account of the electrochemical process by assuming Tafel kinetics at both electrodes.

The present work is concerned with the experimental study of the influence of total current, electrolyte flow rate and type of electrical connection on the current distribution in electrochemical reactors with a gas-evolving electrode. The experimental results are compared with theoretical predictions.

2. Experimental details

2.1. Test reactions

Hydrogen evolution was used as cathodic reaction. The oxidation of sulphite to sulphate from alkaline sodium sulphite solution was chosen as anodic reaction, because it offers a combined diffusion and charge-transfer kinetic control without altering the surface area of the electrode.

The electrochemical oxidation of sulphur dioxide compounds has been investigated by many authors, either to improve the understanding of the reaction mechanism [14], or to obtain an alternative anodic reaction for hydrogen production [15] and other processes [16, 17], or to remove sulphur dioxide from flue gas [18, 19]. However, in all these cases it is carried out with acid solutions and, consequently, with electrodes of graphite, noble metals or their oxides.

Preliminary experiments in this laboratory indicated a maximum anode potential of 1.1 V against Hg/HgO in 0.1 M NaOH and an electrolyte concentration of $170\,g\,dm^{-3}$ Na_2SO_3 and $4\,g\,dm^{-3}$ NaOH for which high current densities were obtained. Under these conditions oxygen evolution was not observed nor was there any attack on the nickel anode. Therefore, in all the experiments, the above electrolyte concentration was used and the maximum potential was not exceeded. In the following, all potentials are quoted with respect to the Hg/HgO in 0.1 M NaOH electrode.

At the same time dithionate can be formed by electrochemical oxidation of sulphite in neutral or alkaline solutions at a platinum anode [20] or PbO_2 anode [21]. However, in this work a nickel anode was polarized at 1.1 V in a conventional three-electrode electrochemical cell and dithionate was not detected [22].

On the other hand, the reduction of sulphur dioxide to dithionite can be expected as a secondary reaction at the cathode [23, 24]. However, for the present case experiments performed in a standard three-electrodes arrangement with a Ni-anode and a Ni-cathode of the same surface area and potentiostating

the anode at 1.1 V showed a hydrogen current efficiency of 100%.

Therefore, for the above electrolyte concentration and up to the maximum anode potential, the electrochemical reactions are only, at the cathode:

$$2H_2O + 2e^- \rightarrow H_2 + 2OH^- \quad (1)$$

and at the anode:

$$SO_3^{2-} + 2OH^- \rightarrow SO_4^{2-} + H_2O + 2e^- \quad (2)$$

Thus it is possible to work with an undivided cell with both electrodes of nickel.

To determine the kinetic parameters of the anodic reaction a rotating nickel disc electrode (5 mm diam.) was used. A similar study was recently performed by Hunger *et al.* [25, 26] for graphite electrodes. The experimental results were correlated employing the usual procedure [27] and assuming the general Levich law for current density, i:

$$1/i = 1/i_k + 1/i_d \quad (3)$$

where i_k is the kinetically limited current density and i_d represents the mass-transfer controlled current density. The following relationship for i_k was obtained:

$$i_k = 6.5 \times 10^{-4} \exp(12.95E) \quad (4)$$

and the diffusion coefficient of sulphite was 1.46×10^{-6} cm^{-2} s^{-1}. Throughout the series of experiments the temperature was maintained at 30 °C for which the kinematic viscosity of the electrolyte was $1{\cdot}15 \times 10^{-2}$ cm^2 s^{-1}.

2.2. Electrochemical reactor

The determinations of the current density distributions were performed in an undivided electrochemical reactor with vertical parallel-plate electrodes, as shown schematically in Fig. 1. The current density distribution was determined employing the segmented electrode method.

The reactor was made of acrylic material with the electrodes of nickel, 200 mm width and 600 mm long, arranged in a filterpress configuration.

The anode was made of 192 squares, 24 mm side and 1 mm thick, arranged in 8 columns of 24 elements. Details of the anode arrangement and data acquisition have been given in an earlier paper [9]. The anode potential was measured and controlled in the lower region, which is the zone of higher potentials. The cathode, a sheet 0.5 mm thick, was electrically fed along its lower edge. A nickel sheet, 1 mm thick, was used as bipolar electrode. The interelectrode gap was 13 mm and, in order to achieve more uniform flow conditions along the electrodes, flow distributor plates with 120 holes of 1.5 mm diameter were arranged in the inlet of the electrolyte and in the outlet of the gas-electrolyte dispersion.

The current distribution for the monopolar case was experimentally determined with this reactor but

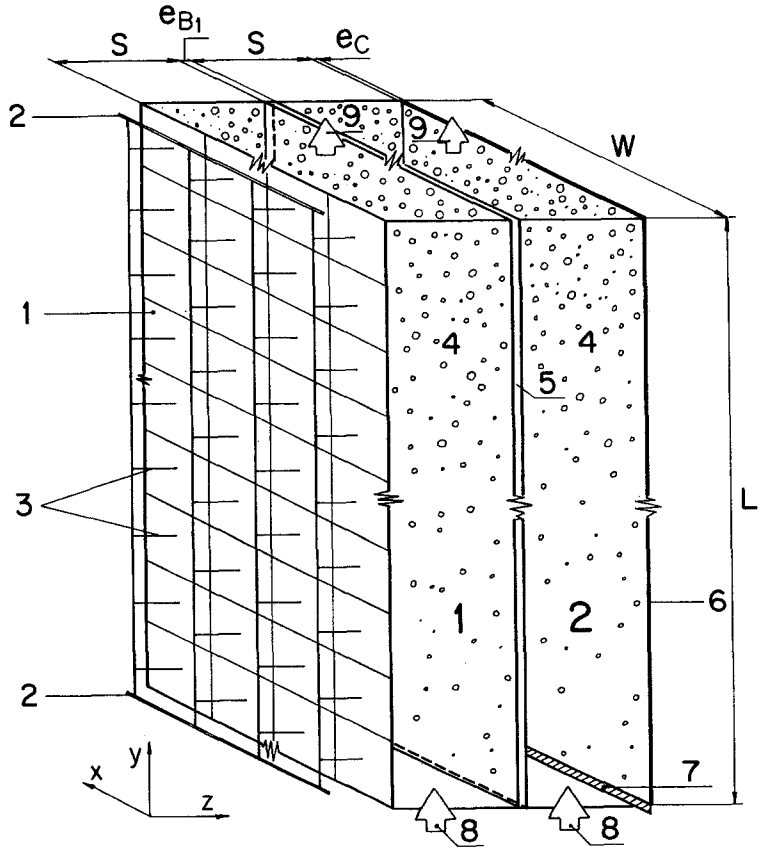

Fig. 1. Schematic representation of the reactor. (1) Segmented anode, (2) anodic current feeder, (3) resistors, (4) solution phase, (5) bipolar electrode, (6) cathode, (7) cathodic current feeder, (8) electrolyte inlets, (9) gas-electrolyte outlets. 1: first reactor; 2: second reactor.

taking out a frame and the bipolar electrode. The reactor was made part of a flow circuit system consisting of a reservoir, a pump, a flowmeter and a gas-liquid separator, with an overall electrolyte volume of 30 dm^3. When the bipolar electrode was used approximately one half of the electrolyte flowed through each cell, due to the symmetrical construction of both cells. The temperature was $30 \pm 2\,^{\circ}C$.

3. Mathematical model

The following model is an extension to electrochemical reactors with bipolar electrodes of the previously reported model [9] for monopolar electrodes. In general, a bipolar electrochemical reactor consists of one anode A, n bipolar electrodes B_n and one cathode C. Each electrode is separated from its neighbour by a thickness S of electrolyte. Therefore, the electrolyte in the gap 1 is in contact with the anode A and the cathodic side of the bipolar electrode B_1 and the electrolyte in the gap $n+1$ is in contact with the anodic side of the bipolar electrode B_n and the cathode C. This geometric configuration has been analysed by Scott [12] assuming that the electrochemical characteristics of each cell can be represented by a pure resistance. In the present work nonlinear electrode kinetic expressions are included in the model and the presence of gas-bubbles in the electrolyte is considered.

The overall voltage balance at the axial position y may be written as

$$V = (n+1)U_0(y) + \Delta\phi_{m,A}(y) + \eta_{a,A}(y) + \Delta\phi_{s,1}(y) + \eta_{c,B_1}(y) + \Delta\phi_{m,B_1}(y) + \cdots + \Delta\phi_m, B_n(y) + \eta_a, B_n(y) + \Delta\phi_{s,n+1}(y) + \eta_{c,C}(y) + \Delta\phi_{m,C}(y) \quad (5)$$

The general Equation 5 is applied to the present reactor with only one bipolar electrode and the following simplifying assumptions are made:

(i) The reversible cell voltage is not a function of y, which is a fair approach because in the Nernst equation large changes in the concentration are necessary to cause an appreciable variation in U_0.
(ii) The thickness of the bipolar electrodes is small with respect to distances in which significant potential variation takes place in the metal phase, so that a one-dimensional model in the y direction is applicable to calculate the potential distribution and therefore the ohmic drops, $\Delta\phi_{m,B_n}$, in the z direction are neglected.
(iii) The ohmic drop in the metal phase of the anode is neglected due to the special construction of the reactor used.
(iv) Current to the cathode is assumed to be fed uniformly over the breadth of the electrode.
(v) In the solution phases the current flows in a direction perpendicular to the electrode surface.
(vi) For each cell, at the axial position y, the bubble distribution is uniform along both the width and the thickness of the compartment, so that the gas voidage varies only in the y direction.
(vii) The reactor is isothermal.

Therefore, Equation 5 becomes

$$\eta_{a,A}(y) + \Delta\phi_{s,1}(y) + \eta_{c,B_1}(y) + \eta_{a,B_1}(y) + \Delta\phi_{s,2}(y) + \eta_{c,C}(y) + \Delta\phi_{m,C}(y) = \text{constant}\,(1) \quad (6)$$

Taking into account the Bruggeman equation to represent the effective electrolyte resistivity, the ohmic drop in the solution phase is given by

$$\Delta\phi_{s,i}(y) = \rho^0[1-\epsilon_i(y)]^{-3/2} S i_i(y) \quad \text{with} \quad i = 1 \text{ or } 2 \quad (7)$$

The ohmic drop in the metal phase of the cathode at the position y is given by

$$\Delta\phi_{m,C}(y) = \frac{\rho_m I}{We_C} y - \frac{\rho_m}{e_C}\int_0^y \int_0^y i_2(y)\,dy\,dy \quad (8)$$

obtained by the integration of the potential equation [28, 29] of the metal phase.

The kinetics of the electrochemical reaction at the cathode are represented by a Tafel law

$$\eta_{c,j}(y) = \frac{1}{b_c}\ln(i_i(y)/i_{0,c}) \quad (9)$$

with $i = 1$ or 2 for $j = B_1$ or C, respectively.

Taking into account Equations 3 and 4 the kinetics of the anodic reaction may be expressed via

$$\eta_{a,j}(y) = -E_{0,a} - \frac{1}{b_a}\ln 6.5 \times 10^{-4} - \frac{1}{b_a}\ln\left[\frac{1}{i_i(y)} - \frac{1}{i_{d,i}(y)}\right] \quad (10)$$

with $i = 1$ or 2 for $j = A$ or B_1, respectively.

The limiting current density is given by

$$i_d = \nu_{e,a} FKC \quad (11)$$

The combined effect of the forced convection and the bubble-induced convection must be taken into account to calculate the mass transfer coefficient. This situation is similar to the interaction between forced convection and natural convection. However, one effect usually predominates in the mass-transfer process and, therefore, Newman [30] recommends that the mass-transfer coefficient for an individual mode of operation must be determined separately and the higher value must be applied.

To calculate the local convective mass-transfer coefficient under developing laminar flow, Pickett [31] gives two main equations. The first approach considers a uniform velocity profile and yields:

$$K_c = \left(\frac{Dv_l^0}{\pi y}\right)^{1/2} \quad (12)$$

Another approximation is provided by boundary layer theory, which gives

$$K_c = 0.332\, D^{2/3}\nu^{-1/6}\left(\frac{v_l^0}{y}\right)^{1/2} \quad (13)$$

The adoption of one of these equations for the modelling will be discussed in detail in Section 4.1.

To calculate the mass-transfer coefficient due to the bubble-induced convection the following equation can be used [32]:

$$K_b = 0.19\left[\frac{D^2 g\epsilon}{\nu(1-\epsilon)}\right]^{1/3} \quad (14)$$

Introducing Equations 7, 8, 9 and 10 into Equation 6 and rearranging yields

$$-\frac{1}{b_a}\ln\left[\frac{1}{i_1(y)}-\frac{1}{i_{d,1}(y)}\right]+\rho^0[1-\epsilon_1(y)]^{-3/2}Si_1(y)$$
$$+\frac{1}{b_c}\ln i_1(y)-\frac{1}{b_a}\ln\left[\frac{1}{i_2(y)}-\frac{1}{i_{d,2}(y)}\right]$$
$$+\rho^0[1-\epsilon_2(y)]^{-3/2}Si_2(y)+\frac{1}{b_c}\ln i_2(y)+\frac{\rho_m I}{We_C}y$$
$$-\frac{\rho_m}{e_C}\int_0^y\int_0^y i_2(y)\,dy\,dy = \text{constant (2)} \quad (15)$$

where the constant (2) is determined by solving Equation 15 at $y = 0$. Thus

$$\text{constant (2)} = \left(\frac{1}{b_a}+\frac{1}{b_c}\right)[\ln i_1(0)+\ln i_2(0)]$$
$$+\rho^0 S[i_1(0)+i_2(0)] \quad (16)$$

The total current I is given by

$$I = W\int_0^L i_1(y)\,dy = W\int_0^L i_2(y)\,dy \quad (17)$$

Another necessary equation is the Kreysa and Kuhn expression [7]

$$\epsilon = \left[\frac{1}{\epsilon_m}+\frac{v_l^0(1-\epsilon/\epsilon_m)}{v_g^0(1-\epsilon)}+\frac{v_{sw}}{v_g^0}\right]^{-1} \quad (18)$$

to describe the gas voidage in the interelectrode gap as a function of position. The gas velocity referred to the cross-section of the cell is given by

$$v_g^0 = \frac{RT}{P\nu_{e,c}FS}\int_0^y i(y)\,dy \quad (19)$$

and the bubble swarm rise velocity is calculated by means of the Richardson–Zaki equation,

$$v_{sw} = v_s(1-\epsilon)^{4.5} \quad (20)$$

However, Equation 15 contains two variables, i.e. $i_1(y)$ and $i_2(y)$, which are related through the potential equation for the metal phase of the bipolar electrode

$$\phi_{m,B_1}(y) = \phi_{m,B_1}(0) - \frac{\rho_m}{e_{B_1}}\int_0^y\int_0^y [i_1(y)-i_2(y)]\,dy\,dy \quad (21)$$

Taking into account Equation 21, Equation 15 can be separated into two contributions, i.e. for the reactor 1:

$$-\frac{1}{b_a}\ln\left[\frac{1}{i_1(y)}-\frac{1}{i_{d,1}(y)}\right]+\rho^0[1-\epsilon_1(y)]^{-3/2}Si_1(y)$$
$$+\frac{1}{b_c}\ln i_1(y)-\frac{\rho_m}{e_{B_1}}\int_0^y\int_0^y$$
$$\times[i_1(y)-i_2(y)]\,dy\,dy = \text{constant (3)} \quad (22)$$

and, for the reactor 2:

$$\frac{\rho_m}{e_{B_1}}\int_0^y\int_0^y[i_1(y)-i_2(y)]\,dy\,dy-\frac{1}{b_a}\ln\left[\frac{1}{i_2(y)}-\frac{1}{i_{d,2}(y)}\right]$$
$$+\rho^0[1-\epsilon_2(y)]^{3/2}Si_2(y)+\frac{1}{b_c}\ln i_2(y)+\frac{\rho_m I}{We_C}y$$
$$-\frac{\rho_m}{e_C}\int_0^y\int_0^y i_2(y)\,dy\,dy = \text{constant (4)} \quad (23)$$

Constant (3) and Constant (4) are evaluated by solving Equations 22 and 23 at $y = 0$, respectively. When the bipolar electrode is isopotential the last

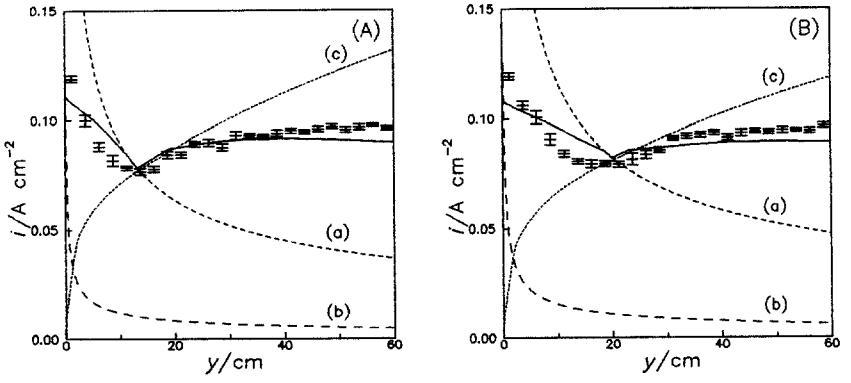

Fig. 2. Current density as a function of the position. Monopolar reactor. (A) $I = 109.87$ A and $Q = 66.67\,cm^3\,s^{-1}$, (B) $I = 109.68$ A and $Q = 112\,cm^3\,s^{-1}$. (a) Limiting current density distribution with the mass-transfer coefficient calculated with Equation 12. (b) Limiting current density distribution with the mass-transfer coefficient calculated with Equation 13. (c) Limiting current density distribution with the mass-transfer coefficient according to bubble-induced convection, Equation 14. Full line: theoretical model. ⊣: Experimental mean value and standard error of the mean.

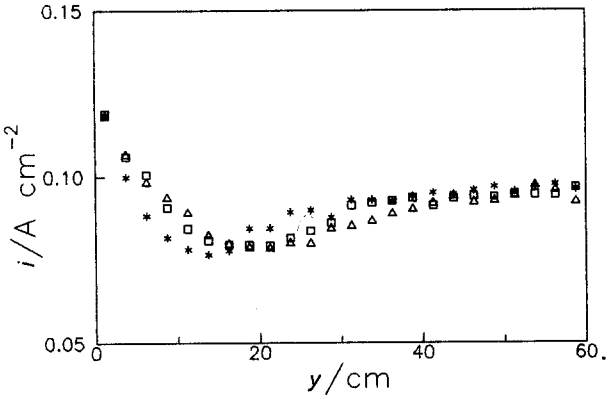

Fig. 3. Effect of the volumetric liquid flow rate on the current density distribution for a given value of total current. Monopolar reactor. (*) $I = 109.87$ A and $Q = 66.67\,\text{cm}^3\,\text{s}^{-1}$, (□) $I = 109.68$ A and $Q = 112\,\text{cm}^3\,\text{s}^{-1}$, (△) $I = 108.86$ A and $Q = 139\,\text{cm}^3\,\text{s}^{-1}$.

term in the left hand side of Equation 22 and the first term in the left hand side of Equation 23 can be neglected.

A simplified model results from the assumption that both reactors have the same current density distribution, thus

$$i_1(y) = i_2(y) \qquad \text{for all } y \tag{24}$$

Therefore for this simplified case, Equation 15 is reduced to

$$-\frac{2}{b_a}\ln\left[\frac{1}{i(y)} - \frac{1}{i_d(y)}\right] + 2\rho^0[1-\epsilon(y)]^{-3/2}Si(y) + \frac{2}{b_c}\ln i(y) + \frac{\rho_m I}{We_C}y - \frac{\rho_m}{e_C} \times \int_0^y \int_0^y i(y)\,dy\,dy = \text{constant (2)} \tag{25}$$

Equation 25 is very similar to that developed for monopolar reactors [9]. The only difference between them is that for the bipolar case the terms for overpotential and ohmic drops in the solution phase are multiplied by the number of reactors in series, two in the present case. The method of calculation has been reported previously [9]. When Equation 25 is used to design bipolar reactors, only the additive effect of the overpotentials and electrolyte ohmic drops on the current distribution are considered.

Table 1. Values of model parameters

ρ^0	8.83Ω cm	S	1.3 cm
ϵ_m	0.38	b_a	12.95 V^{-1}
v_s	3.5 cm s^{-1}	b_c	25.58 V^{-1}
ρ_m	7.41 × 10^{-6} Ω cm	$\nu_{e,a}$	2
L	60 cm	$\nu_{e,c}$	2
W	20 cm	D	1.46 × 10^{-6} cm^2 s^{-1}
e_{B_i}	0.1 cm	ν	1.15 × 10^{-2} cm^2 s^{-1}
e_C	0.05 cm	g	980.66 cm s^{-2}

A more realistic situation is to also take into account the effect of the metal phase of the bipolar electrode. For this it is necessary to solve simultaneously Equations 22 and 23. Therefore, in this work a current distribution was initially assumed for reactor 1 and the current distribution for reactor 2, $i_2(y)$ was calculated using Equation 23. Then the current distribution for reactor 1 was calculated using $i_2(y)$ and Equation 22. This procedure was repeated until agreement was achieved between the assumed distribution and that calculated for each reactor. In Section 4.2 the results of this calculation method are given and compared with the predictions of the simplified model, i.e. Equation 25.

4. Results and discussion

4.1. Monopolar electrodes

Figure 2 shows typical experimental current density distributions. Each point is the mean value of the eight columns for a given value of y and the vertical bar represents the standard error of the mean.

In the first half of the reactor a pronounced current distribution occurs with a minimum at a distance from the inlet region approximately six times the equivalent diameter of the reactor. The minimum position depends on the total current and on the volumetric liquid flow rate. This minimum is produced by the interaction between the forced convection and the bubble-induced convection. The forced convection dominates the inlet region and its local mass-transfer coefficient decreases, according to Equations 12 or 13, with the $-1/2$th power of y. In contrast, the local mass-transfer coefficient due to the bubble-induced

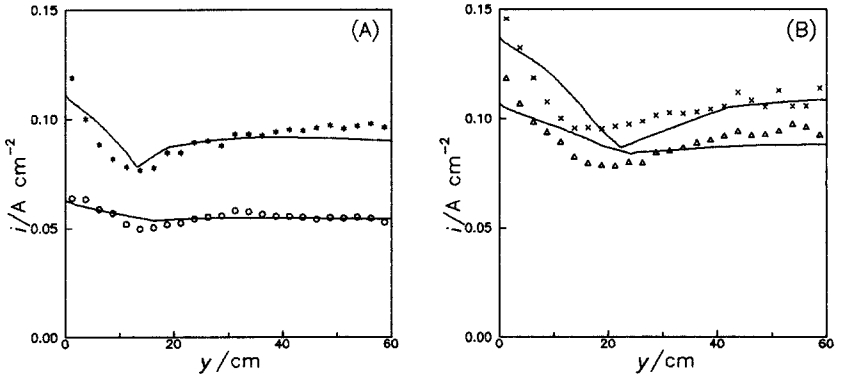

Fig. 4. Effect of the total current on the current density distribution for a given value of the volumetric liquid flow rate. Monopolar reactor. (A) $Q = 66.67\,\text{cm}^3\,\text{s}^{-1}$, (B) $Q = 139\,\text{cm}^3\,\text{s}^{-1}$. (○) 66.20 A, (*) 109.87 A, (△) 108.86 A, (×) 128.23 A.

Table 2. Results obtained for the monopolar electrochemical reactor

Fig.	*Curve*	*I*/A	Q/cm^3 s^{-1}	$\bar{\delta}_r \times 10^2$
4	A (○)	66.20	66.67	2.81
2 and 4	A and A (∗)	109.87	66.67	5.27
2	B	109.68	112	6.25
4	B (△)	108.86	139	7.00
4	B (×)	128.23	139	5.88

Table 3. Results obtained for the bipolar electrochemical reactor

Fig.	*Curve*	*I*/A	Q/cm^3 s^{-1}	$\bar{\delta}_r \times 10^2$
5	A (∗)	66.07	112	2.2
5	A (○)	104.94	112	5.66
5	A (+)	129.95	112	6.08
5	B (△)	49	133.33	3.91
5	B (□)	61.16	133.33	5.2
5	B (◇)	79.33	133.33	6.97
5	B (×)	101.11	133.33	6.94

convection increases, at a vertical electrode, with y. This results in a minimum in the current distribution because the anodic reaction is influenced by the mass-transfer.

In order to determine for the present reactor the validity of Equations 12 or 13, in Fig. 2 the limiting current density distributions with the mass-transfer coefficient calculated according to both equations are represented by the dashed line. It is observed that in the inlet region the limiting current densities predicted by Equation 13, curve b, are lower than the experimental current densities. Therefore Equation 13 is inadequate for the present case and Equation 12 was adopted for the modelling.

In Fig. 2 the limiting current density distribution taking into account only the bubble-induced convection, curve c, is also included. The mass-transfer coefficient was calculated using Equation 14 and the experimental current distribution was considered to evaluate the gas voidage. It can be seen that beyond the minimum in the current distribution the bubble-induced convection dominates the mass-transfer.

In the second half of the reactor the current distribution is mainly influenced by the effect of gas-bubbles on the electrolyte resistivity and, likewise, by the resistance of the metal phase, which causes the current distribution to be more even.

The full line in Fig. 2 represents the theoretical current distribution. The parameters given in Table 1 were used. It is observed that there is a close agreement with the experimental results. The largest deviations are found in the inlet region of the reactor because the convective coefficient was calculated using Equation 12 and the effect of the change of flow area on the mass transfer conditions [33–35] was neglected.

Figure 3 shows the influence of the volumetric liquid flow rate on the current distribution for a given current. It is observed that the position of the minimum moves away from the inlet region as the flow rate increases due to the increase in the convective mass-transfer coefficient.

Figure 4 shows the influence of the total current on the current distribution for a given value of the volumetric liquid flow rate. In contrast to the preceding case the minimum moves near to the inlet region when the total current increases, due to the increase in the bubble-induced mass-transfer coefficient. Likewise, the current distribution is more uneven when the current increases. The full lines in Figs 2 and 4 correspond to the theoretical model and in Table 2 the mean relative deviation for each case is given. It can be seen that the agreement between the theoretical and experimental results is better when the volumetric liquid flow rate is lower, probably due to the difficulty in calculating exactly the convective mass-transfer coefficient.

4.2. Bipolar electrode

Figure 5 shows some typical experimental current density distributions for the electrochemical reactor with a bipolar electrode for different values of total current and volumetric liquid flow rate. The full lines correspond to the theoretical model assuming that both reactors have the same current density distributions, Equation 25. Table 3 summarizes these

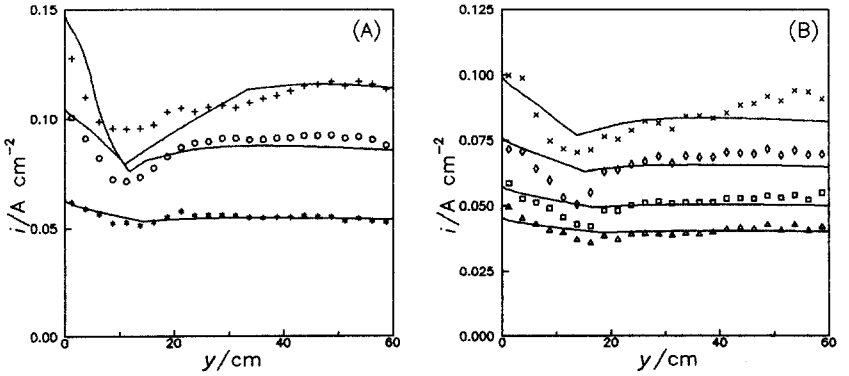

Fig. 5. Current distribution as a function of the position for the electrochemical reactor with a bipolar electrode. (A) $Q = 112\,\text{cm}^3\,\text{s}^{-1}$, (B) $Q = 133.33\,\text{cm}^3\,\text{s}^{-1}$. (∗) 66.07 A, (○) 104.94 A, (+) 129.95 A, (△) 49A, (□) 61.16 A, (◇) 79.33 A, (×) 101.11 A. Full lines: simplified model, Equation 25.

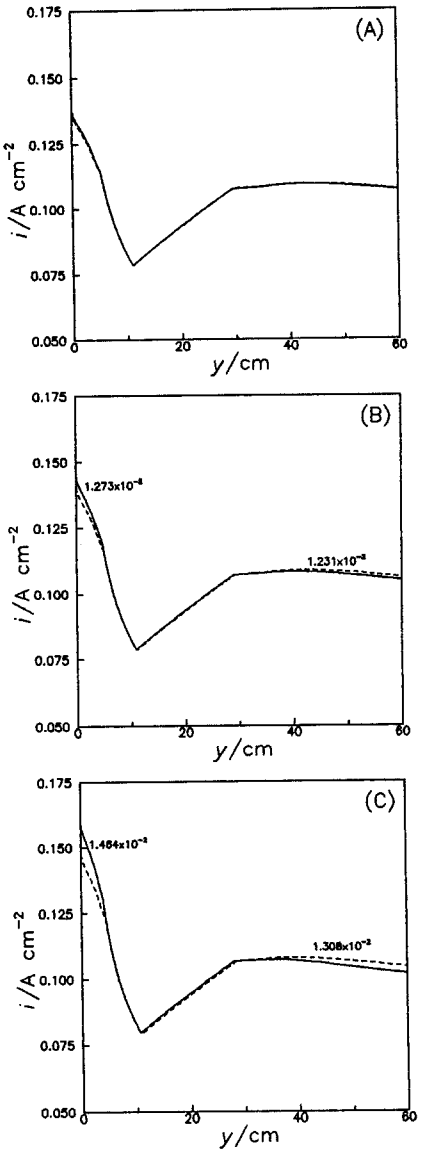

Fig. 6. Comparison of the current density distributions for the monopolar and bipolar cases for different resistance values of the terminal electrode. Full line: monopolar reactor. Dashed line: bipolar stack according to the simplified model. $I = 125\,\text{A}$ and $Q_{\text{reactor}} = 56\,\text{cm}^3\,\text{s}^{-1}$. (A) $e_c = 0.05\,\text{cm}$, and $\rho_m = 7.41 \times 10^{-6}\,\Omega\,\text{cm}$. (B) $e_C = 0.01\,\text{cm}$ and $\rho_m = 7.41 \times 10^{-6}\,\Omega\,\text{cm}$. (C) $e_C = 0.05\,\text{cm}$ and $\rho_m = 10^{-4}\,\Omega\,\text{cm}$. Other parameters according to Table 1.

results and it is observed that the mean relative deviation is always lower than 7% which shows that the mathematical model is reliable for design of such reactors. It is also noted that $\bar{\delta}_r$ is slightly higher for the bipolar case than for the monopolar case and, in general, $\bar{\delta}_r$ increases when the current or the volumetric liquid flow rate increases.

To analyse the effect of the metal phase resistance of the terminal electrode on the current distribution, theoretical current density distributions are represented in Fig. 6 for the monopolar reactor and for the bipolar stack according to the simplified model, Equation 25. The full line corresponds to the monopolar case and the dashed line to the bipolar one and the number on each curve represents the population standard deviation, σ. It is observed in Fig. 6(A) that when the metal resistance is low, corresponding to the studied experimental reactor,

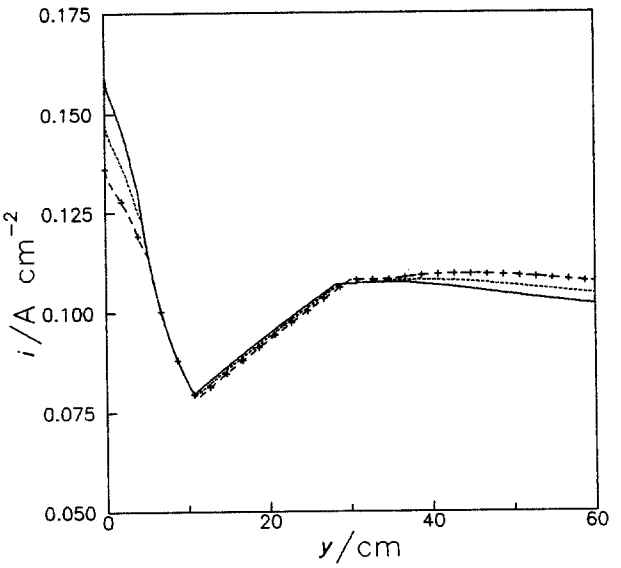

Fig. 7. Effect of the terminal electrode resistance on the current distribution in a bipolar stack with two reactors. Full line: reactor 2. Dashed line: reactor 1. Dotted line: simplified bipolar model. (+) current distribution for a monopolar reactor with isopotential electrodes. $I = 125\,\text{A}$, $Q = 112\,\text{cm}^3\,\text{s}^{-1}$, $e_C = 0.05\,\text{cm}$ and $\rho_m = 10^{-4}\,\Omega\,\text{cm}$. Other parameters according to Table 1.

the current distribution at each electrode of the bipolar stack is very similar to those for the monopolar reactor. However, when the resistance of the metal phase increases, (higher resistivity or lower electrode thickness), the bipolar stack gives a more uniform current distribution, (lower value of σ). The current densities before the minimum in the bipolar stack are lower than those in the monopolar reactor and the inverse situation is noted beyond the minimum value. This occurs because in the bipolar case the solution resistance is higher than that for the monopolar reactor, which diminishes the current distribution in the region of higher current densities, *viz.* the feeder region. Thus, in order to reach the given value of total current the current densities are higher in the second half of the bipolar reactor.

In Fig. 7 the current distributions for a bipolar stack with two reactors are compared according to the simplified model, Equation 25, and the rigorous model, Equations 22 and 23. The curve of the simplified model, dotted line, is the same as in Fig. 6(C). It is observed that when the reactor has a resistive terminal electrode both models predict very different current density distributions. According to the rigorous model the reactor 2 presents a sharped current distribution because of the high metal resistance of the terminal electrode. However, the current distribution in reactor 1 is smoothed due to the combined effect of the solution resistance and the presence of the bipolar electrode.

In Fig. 7 the symbols (+) represent the current distribution for a monopolar reactor with isopotential electrodes, $\rho_m = 0$. In this case the current distribution is mainly imposed by the variation of the mass-transfer coefficient along the reactor. It must be noted that for the bipolar stack the

reactor 1 has the same current density distribution as a monopolar reactor with isopotential electrodes in spite of the sharp current distribution of reactor 2. Thus, the metal phase of the terminal electrode influences the current distribution only in the reactor with the resistive terminal electrode. It is important to take into account this behaviour in the design of the current feeders for bipolar stacks.

5. Conclusions

From this work, the following conclusions may be drawn:

(i) The agreement between the experimental and theoretical current distributions are close, therefore the model is appropriate for the design of monopolar as well as bipolar reactors.
(ii) The current density distribution shows a minimum, which is a consequence of the changes in the mass-transfer coefficient along the reactor due to the combined effects of forced convection and bubble-induced convection.
(iii) In a bipolar stack, when the terminal electrodes are isopotential, all the reactors have the same current density distribution.
(iv) Terminal resistive electrodes in a bipolar stack only influence the current density distribution at the outermost cells of the stack.
(v) For the calculation of the current distribution in a bipolar stack it is more convenient to solve the voltage balance equation for each reactor of the stack instead of solving the overall voltage balance.

References

[1] C. W. Tobias, *J. Electrochem. Soc.* **106** (1959) 833.
[2] J. E. Funk and J. F. Thorpe, *ibid.* **116** (1969) 48.
[3] Y. Nishiki, K. Aoki, K. Tokuda and H. Matsuda, *J. Appl. Electrochem.* **16** (1986) 615.
[4] I. Rousar, V. Cezner and J. Hostomsky, *Collect. Czech, Chem. Commun.* **36** (1971) 1.
[5] I. Rousar, V. Cezner, J. Nejepsova, M. M. Jacksic, M. Spasojevic and B. Z. Nikolic, *J. Appl. Electrochem.* **7** (1977) 427.
[6] I. Rousar, *J. Electrochem. Soc.* **116** (1969) 676.
[7] G. Kreysa and M. Kuhn, *J. Appl. Electrochem.* **15** (1985) 517.
[8] A. D. Martin and A. A. Wragg, *J. Appl. Electrochem.* **19** (1989) 657.
[9] J. M. Bisang, *ibid.* **21** (1991) 760.
[10] L. J. J. Janssen and C. J. Visser, *ibid.* **21** (1991) 753.
[11] L. R. Czarnetzki and L. J. J. Janssen, *ibid.* **19** (1989) 630.
[12] K. Scott, *Electrochim. Acta* **28** (1983) 133.
[13] J. Divisek, *J. Appl. Electrochem.* **14** (1984) 663.
[14] A. J. Appleby and B. Pichon, *J. Electroanal. Chem.* **95** (1979) 59.
[15] P. W. T. Lu and R. L. Ammon, *J. Electrochem. Soc.* **127** (1980) 2610.
[16] D. P. Ziegler, M. Dubrovsky and J. W. Evans, *J. Appl. Electrochem.* **11** (1981) 625.
[17] K. A. Spring and J. W. Evans, Energy Reduct. Tech. Met. Electrochem. Processes, Proc. Symp. (1985) p. 309.
[18] G. Kreysa, *DECHEMA-Monogr.* **109** (1987) 9.
[19] G. Kreysa, J. M. Bisang, W. Kochanek and G. Linzbach, *J. Appl. Electrochem.* **15** (1985) 639.
[20] S. I. Zhdanov, *in* 'Standard Potentials in Aqueous Solution' (edited by A. J. Bard, R. Parsons and J. Jordan), Marcel Dekker, New York (1985) chapter 6, pp. 103.
[21] G. Cohn, *in* 'Enciclopedia de Química Industrial' (directed by F. Ullmann), Gustavo Gilli, Buenos Aires (1932), Section II, pp. 222.
[22] G. Charlot, 'L'Analyse Qualitative et les Réactions en Solution', Masson, Paris (1963), chapter 12, pp. 374.
[23] C. Oloman, *J. Electrochem. Soc.* **117** (1970) 1604.
[24] C. Oloman, B. Lee and W. Leyten, *Can. J. Chem. Eng.* **68** (1990) 1004.
[25] T. Hunger and F. Lapicque, *Electrochim. Acta* **36** (1991) 1073.
[26] T. Hunger, F. Lapicque and A. Storck, *J. Appl. Electrochem.* **21** (1991) 588.
[27] A. J. Bard and L. R. Faulkner, 'Electrochemical Methods. Fundamentals and Applications', John Wiley & Sons, New York (1980) chapter 8, pp. 290.
[28] J. M. Bisang and G. Kreysa, *J. Appl. Electrochem.* **18** (1988) 422.
[29] J. M. Bisang, *Lat. Am. Appl. Res.* **18** (1988) 63.
[30] J. S. Newman, 'Electrochemical Systems', Prentice Hall, Englewood, Cliffs, NJ (1973), chapter 17, pp. 330.
[31] D. J. Pickett, 'Electrochemical Reactor Design', 2nd edn, Elsevier Scientific, Amsterdam (1979) chapter 4, p. 134.
[32] L. Sigrist, O. Dossenbach and N. Ibl, *Int. J. Heat Mass Transfer* **22** (1979) 1393.
[33] A. A. Wragg, D. J. Tagg and M. A. Patrick, *J. Appl. Electrochem.* **10** (1980) 43.
[34] D. J. Pickett and C. J. Wilson, *Electrochim. Acta* **27** (1982) 591.
[35] D. F. Fletcher, S. J. Maskell and M. A. Patrick, *Comput. Fluids* **13** (1985) 207.